Article

Study of Plasma Electrolytic Oxidation Coatings on Aluminum Composites

Leonid Agureev [1], Svetlana Savushkina [1,2], Artem Ashmarin [1], Anatoly Borisov [2,*], Andrey Apelfeld [2] , Kirill Anikin [2], Nikita Tkachenko [3], Mikhail Gerasimov [4], Aleksandr Shcherbakov [4], Vasily Ignatenko [4] and Natalia Bogdashkina [4]

[1] Department of Nanotechnology, Keldysh Research Center, 125438 Moscow, Russia; trynano@gmail.com (L.A.); sveta_049@mail.ru (S.S.); ashmarin_artem@list.ru (A.A.)

[2] Moscow Aviation Institute (National Research University), 121552 Moscow, Russia; apelfeld@yandex.ru (A.A.); airgear12@mail.ru (K.A.)

[3] Skobel'tsyn Institute of Nuclear Physics, Moscow State University, 11999 Moscow, Russia; nicki_tkak@mail.ru

[4] Institute of Physical Chemistry and Electrochemistry of RAS, 119991 Moscow, Russia; mvger2018@yandex.ru (M.G.); schebakov@ipc.rssi.ru (A.S.); basil148@mail.ru (V.I.); bogdnat45@yandex.ru (N.B.)

* Correspondence: anatoly_borisov@mail.ru; Tel.: +7-495-353-8334

Abstract: Coatings, with a thickness of up to 75 μm, were formed by plasma electrolytic oxidation (PEO) under the alternating current electrical mode in a silicate-alkaline electrolyte on aluminum composites without additives and alloyed with copper (1–4.5%). The coatings' structure was analyzed by scanning electron microscopy, X-ray microanalysis, X-ray photoelectron spectroscopy, nuclear backscattering spectrometry, and XRD analysis. The coatings formed for 60 min were characterized by excessive aluminum content and the presence of low-temperature modifications of alumina γ-Al_2O_3 and η-Al_2O_3. The coatings formed for 180 min additionally contained high-temperature corundum α-Al_2O_3, and aluminum inclusions were absent. The electrochemical behavior of coated composites and uncoated ones in 3% NaCl was studied. Alloyage of aluminum composites with copper increased the corrosion current density. Plasma electrolytic oxidation reduced it several times.

1. Introduction

Powder aluminum composites are promising construction materials due to their low weight, low costs, and high specific strength [1–3]. Several methods to improve their strength properties have been developed (copper alloying, modification by nanoparticle additives, etc.) that allow tensile strength to increase the by up to 630 MPa [3–6].

Aluminum alloys with copper have high strength. However, with increasing copper concentration, the corrosion resistance decreases, which is shown in a number of works [7–9] for the alloys: Powder alloy Al + 1–2% Cu, age-hardenable alloys 2011-T3, AA2024-T4, AA7075-T651, AA7475-T761, and experimental alloy Al + 5% Cu. This is mainly because the $CuAl_2$ intermetallic compound formed during heat treatment promotes corrosion, playing the role of a cathode inclusion in these processes. In this connection, it is important to develop methods for corrosion protection of aluminum based composites alloyed with copper. Another important problem is increasing their wear resistance.

These problems can be solved by the formation of ceramic-like coatings by plasma electrolytic oxidation (PEO) [10–12]. It is known that PEO coatings have high corrosion-protective ability, wear

resistance, and heat resistance [10–19]. PEO technology is well developed for compact aluminum alloys. PEO coatings on such alloys are characterized by a layered structure. A thin transition layer at the boundary with the substrate is responsible for its corrosion-protective properties. The main layer of PEO coatings on aluminum alloys, generally, includes the corundum, α-Al_2O_3, which has high microhardness and provides good wear resistance [10,11,18–21]. In particular, aluminum alloys with PEO coatings have a high wear resistance under sliding friction [22–27].

The objectives of this study were the synthesis of PEO coatings on aluminum composites (without additives and alloyed with copper) and the investigation of their structure and properties. It can be assumed that, in materials consisting of grains with surface oxide films (such as aluminum composites), the sequential oxidation of microvolumes will occur during the PEO process. It may affect the course of the PEO treatment process and the coating structure. For example, during the PEO coating formation on aluminum, which was preliminarily prepared by anodizing oxide film, the voltage decreases at the initial stage of the process and the fragments of anode film are presented in the coating structure [28]. The structure and properties of PEO coatings on composites can differ from those on compact alloys. So, the negative effect of the strengthening phase on the corrosion and wear resistance of formed oxide coatings was shown in [29], which focused on the PEO treatment of magnesium-based composites hardened by SiC particles. In [30], compact ceramic coatings were fabricated on a SiCp/A356 aluminum composite surface by PEO. The results showed that the SiCp hinders the coating growth, but that the coating integrity is not disrupted. At the initial PEO stage, outward-growth dominates the growth behavior of the coatings in the total thickness. Starting from 30 min, the total thickness of the coatings increases gradually and the total growth rate declines sharply. At this stage, the outward growth gradually slows down and the inward growth maintains persistent enhancement. During the PEO process the oxide coating is mainly composed of γ-Al_2O_3 at the initial stage and composed of γ-Al_2O_3, α-Al_2O_3 and mullite after 20 min. The ceramic coating showed good wear and excellent corrosion resistance. In [31], oxide ceramic protective coatings produced by PEO in a silicate-alkaline electrolyte under the AC electrical mode on aluminum matrix composites processed by powder metallurgy using alloy EN AW 2017 and SiC or Al_2O_3, particles were investigated to solve the problem of fatigue wear. It was also shown that compactness and thickness were not deteriorated by the incorporation of thermodynamically stable alumina particles. The decomposition of silica particles during the PEO processes caused an increase of the coating porosity. Nevertheless, there are many unstudied issues related to the plasma electrolytic oxidation of aluminum composites.

2. Materials and Methods

Samples of powdered aluminum composites without additives (Al) and those alloyed with copper from 1% to 4.5% Cu (Al + 1%; 2%; 3%; 4%; 4.5% Cu) were prepared by the powder metallurgy methods of cold pressing and subsequent sintering in vacuum. The aluminum powder with an average particle size of 4 μm was used as a matrix. The copper powder, with an average particle size of about 2 μm, was used for alloying. Aluminum powder was sieved with a cell of 14 microns, then mixed with copper powder in a ball mill, with a balls to powder ratio of 1:4, in hexane, and placed in an ultrasonic bath (20 kHz), while stirring the mixture by a rotary stirrer (400 rpm). Drying of suspension took place in air at 60 °C for 24 h. The resulting blend was compressed into a cylindrical mold with a pressure of 400 MPa. A hydraulic press and a cylindrical mold were used for pressing (diameter 14 mm, height 17 mm). Sintering was carried out in a low-vacuum furnace at a temperature of 650 °C for 180 min. The density of composites, measured by the hydrostatic method, varied from 2.50 for Al to 2.63 g/cm^3 for the Al + 4.5% Cu composite. The total porosity of the composites calculated from these data ranged from 8 to 5%, respectively.

PEO coatings were formed in silicate-alkaline electrolyte containing 2 g/L of potassium hydroxide and 9 g/L of sodium silicate. PEO treatment was carried out under the AC electrical mode (50 Hz) at equal values of anode and cathode currents and total current density of 12.5 A/dm^2. The PEO duration was 60, 90 and 180 min.

The thickness of the PEO coatings was measured on the samples' cross-sections by a scanning electron microscope (SEM, FEI Company, Eindhoven, Netherlands), Quanta 600. The surface and cross-sections' structure and the elemental composition of the PEO coatings were studied using SEM and energy-dispersive (EDX) X-ray microanalysis, TRIDENT XM 4 (the energy of accelerated electrons—20 keV). The composition of the coatings' surface layer was studied by X-ray photoelectron spectrometry (XPS, PHI, USA) using a spectrometer Quantera. Before analysis, the researched areas of the coatings were purified by argon ions, with an energy of 2 keV. The elemental depth profile of the coatings was nondestructively determined by proton nuclear backscattering (NBS) spectrometry using the 120 cm cyclotron of the Skobeltsyn Institute of Nuclear Physics of Moscow State University [13,32]. The proton-beam energy was 7.4 MeV, the beam diameter was 3 mm, and the scattering angle was 160°. Similar to the well-known Rutherford backscattering spectrometry [33], NBS-spectrometry enables depth profiling of elemental composition, but is more sensitive to light elements (C, N, O). The NBS analysis depth reaches 100 µm. The phase composition was examined using an X-ray diffractometer (Empyrean PANalytical) in CuKα radiation. The hardness of the coatings was measured on the microhardness tester, Micromet 5114, with a load on indenter of 0.25 N. The time from the start of the load application to its nominal value was 5 s. The exposure under the load was 10 s.

Electrochemical studies were carried out for Al and Al + 1; 2; 3% Cu composites both with PEO coating and without coating. The corrosion solution was prepared with chemically pure NaCl. All experiments were carried out in a standard three-electrode cell using the IPC PRO L potentiostat. Polarization of samples was carried out from the cathode region to the anode one in 3% NaCl solution at a potential sweep rate of 1 mV/s. The polarization experiments were conducted thrice for the various aluminum composites.

3. Results

3.1. PEO Voltage-Time Response and the Thickness of the Coatings

The thickness of PEO coatings formed in result of 60 min of PEO treatment on Al composite was 40 µm. When the duration of the PEO was increased to 180 min, the coating thickness on the Al composite without alloying additives reached 75 µm.

The copper additives into aluminum composites in the amount of 1% to 4.5% affected the composition and structure of the coatings and changed the voltage-time dependencies of the PEO process. Visually, the coatings changed color from white for pure Al composite and to brown for composites with copper. The PEO process voltage-time response shows (Figure 1) that the anode voltage for the Al + 1% Cu composite was slightly higher than the voltage for the pure Al composite, which resulted in a 5 µm thicker coating (~45 µm). With the increasing of the copper content in the composite to 4.5%, the voltage rise slowed at the initial stage of the PEO, which is associated with the formation of the barrier oxide layer. As a result, the PEO coating formed for 60 min on the composite, Al + 4.5% Cu, was characterized by an inhomogeneous thickness with an average value of 25 µm.

3.2. Surface and Cross-Section Microstructure of PEO Coatings

SEM showed that the average particles size of the composites was about 5 µm (Figure 2a). The surface morphology of the PEO coatings on composites was similar to that of the coatings on compact aluminum alloys (Figure 2b) [10]. It was characterized by crater-like regions of alumina and areas enriched by electrolyte components. The size of alumina craters reached 30 µm. The increase in the concentration of copper of up to 4.5% in aluminum composites led to an increase in the size of the craters (Figure 2c) and areas enriched by electrolyte components.
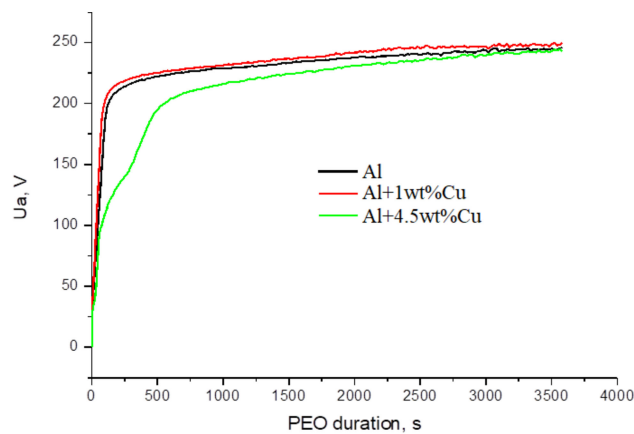
Figure 1. Voltage-time response of the anode voltage, *U*a, for the composites: Al; Al + 1% Cu; Al + 4.5% Cu.
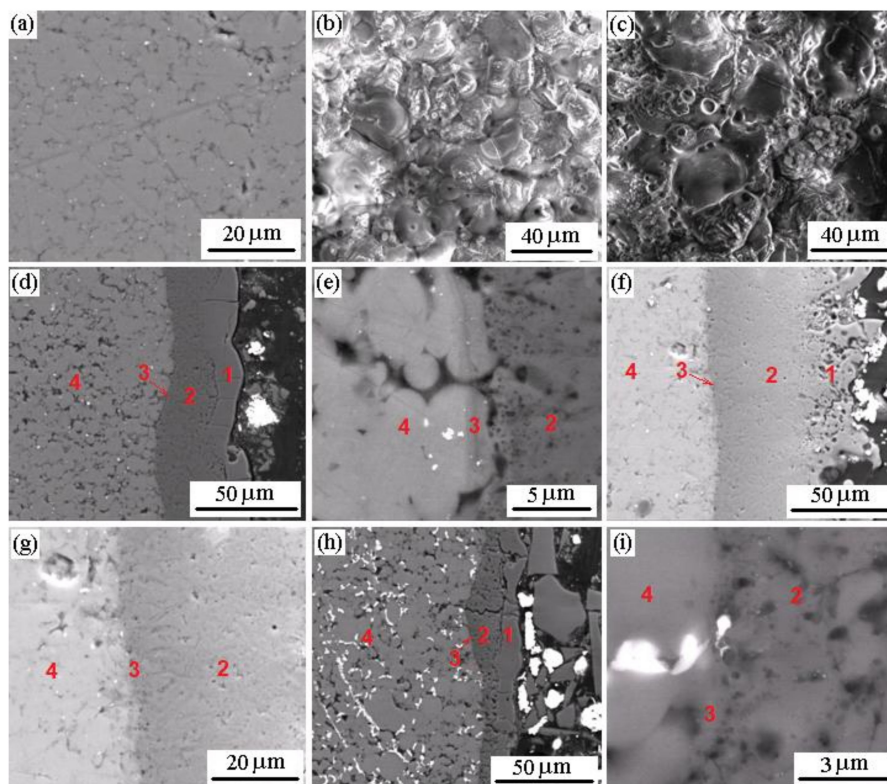
Figure 2. The backscattered electron image of the initial structure of the composite Al (**a**); the secondary electron images of PEO coatings on the composite Al (**b**) and the composite Al + 4.5% Cu (**c**); the backscattered electron images of the cross-section of the coating on the composite Al after 60 mins of PEO treatment (**d**) and its barrier layer (**e**); the coating on the composite Al after 180 mins of PEO treatment (**f**) and its barrier layer (**g**); the coating on the composite Al + 4.5% Cu (**h**) after 60 mins of PEO treatment and its barrier layer (**i**). 1—outer layer; 2—main layer; 3—transition (barrier) layer; 4—composite.

Studies of the cross-sections of the PEO coatings on aluminum composites showed the presence of three layers: A transition (barrier) layer at the boundary with the composite, with a thickness of about 0.5 μm; a main (inner) layer; and an outer layer [10,16]. The structures of PEO coatings on Al and Al + 1% Cu composites were almost identical. The difference in thickness corresponded to an average particle size of the composite of ~5 μm. With a total thickness of about 40 μm, the thickness of the outer layer was about 15 μm (Figure 2d). Its structure was characterized by separate crater channels that

penetrate the layer and remained in the coating after the end of the microdischarges' burning. The main layer had a grained structure. Its porosity increased when approaching the transition layer (Figure 2e). This may be due to the influence of the primary porosity of aluminum composites. The structure of the coating near the barrier layer had its own characteristics. In Figure 2e, it is seen that the barrier layer is "deepened" relative to the PEO coating on ~1 μm in the composite structure. This may be due to the slowing down of the PEO process in result of consecutive processing of the composite grains, first, from the outside side and incorporation of them into the coating, with the metal center maintaining and following their complete oxidation.

When the PEO duration was 180 min the coating thickness on the Al composite without alloying additives reached ~75 μm (Figure 2f). The outer layer became more porous, but the porosity at the barrier layer boundary decreased (Figure 2g).

Figure 2h shows the cross-sectional structure of the Al + 4.5% Cu composite with the PEO coating. It is seen that copper-containing lamellar phases (presumably θ'-$CuAl_2$) of up to ~3 μm in size are located along the composite particles boundaries. The total thickness of the coating varies from 16 to 40 μm. The thickness of the outer layer in some areas reached ~20 μm and exceeds the thickness of the main layer. When the transition layer approaches the copper-containing islands, they are gradually built into the structure of the coating, presumably, as inclusions of copper oxide (Figure 2i).

3.3. XPS Data

The elemental composition of the PEO coatings' surface was studied by X-ray photoelectron spectroscopy. An example of the XPS spectrum for the Al + 1% Cu composite is shown in Figure 3. To estimate the chemical composition of the coatings, the photoelectron peaks were approximated by Gaussian and Lorentz functions.
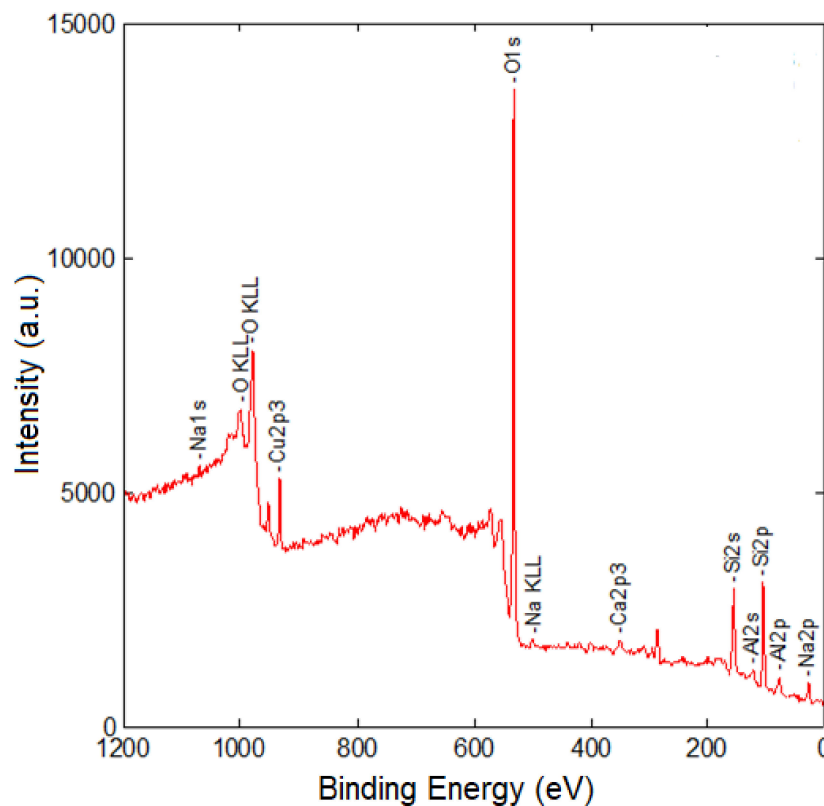
Figure 3. X-ray photoelectron spectrum of the PEO coating on the composite Al + 1% Cu.

XPS showed that oxygen (~70 at %) and silicon (~19 at %) predominate in the surface layer of PEO coatings on the Al composite (Table 1). The aluminum content was only about 9% and Na and K were also detected (less than 1%). In the Al + 1% Cu composite, the copper content in the surface layer of PEO coatings was about 0.7%, while, in the composite Al + 4.5% Cu, it was about 2% (Figure 3). Silicon, potassium, and sodium are elements of the electrolyte components and can be incorporated into the coating during the PEO process in the form of oxides, including complex ones.

Decomposition of the Al and Si peaks revealed the presence of Al_2O_3, SiO_2, Al_2SiO_5, and $NaAlSi_3O_8$ phases in the surface layer of PEO coating.

Table 1. XPS Data.

Composite	Element, at %						
	O	**Si**	**Al**	**Na**	**Ca**	**Cu**	**K**
Al	70	19	9	<1	2	-	<1
Al + 1% Cu	70	21	6	<1	1	1	<1
Al + 4.5% Cu	67	22	8	<1	1	2	<1

3.4. EDX Data

In the outer layer of the PEO coatings on Al composite X-ray microanalysis revealed, in addition to the elements of the alumina phase (Al ~42 at % and O ~57%), the presence of about 1% of Si, which is an element of the electrolyte component (sodium silicate) and can be incorporated into the coating at complex oxide formation. It can be assumed that microarc discharges involve the electrolyte, Na_2SiO_3, molecules, which, after plasma treatment in the discharge channel, form mullite and SiO_2. The main layer of PEO coatings consisted of aluminum and oxygen, but was characterized by an elevated aluminum content (~45 at %).

The outer layer of the PEO coatings on the Al + 4.5% Cu composite contained ~41% of Al; 56% of O; 1% of Si, and 2% of Cu. In the main coating layer, there was 43% of Al; 56% of O; 1% of Si, and up to 2% of Cu. Cu and Si are, probably, present in the form of an oxides. A summary of the results is given in Table 2.

Table 2. EDX Data.

Composite	Layer	Element, at %			
		Al	**O**	**Si**	**Cu**
Al	Outer layer	42	57	1	-
	Main layer	45	54	-	-
Al + 1% Cu	Outer layer	41	58	1	-
	Main layer	42	58	1	-
Al + 4.5% Cu	Outer layer	41	56	1	2
	Main layer	43	56	1	1

3.5. NBS Data

To determine the ratio of aluminum to oxygen in the PEO coatings an elemental analysis was performed using proton nuclear backscattering spectrometry. Figure 4 shows the energy spectrum of backscattered protons for the PEO coating with a thickness of ~45 μm on the Al + 1% Cu composite as recorded by a multichannel energy analyzer. The initial proton energy of 7.4 MeV corresponded to the 250th channel of the analyzer. The scattering of protons on the atomic nuclei in the surface layer of the coating corresponded to the right edges of the spectrum peaks, with the largest values of the proton energy elastically scattered on the Al atoms (~230th channel) and O atoms (~210th channel). The left parts of the spectrum peaks correspond to the scattering of protons by atomic nuclei on the

inner layer of the coating. The width of the peaks was determined by the thickness of atoms layer where this element is present.
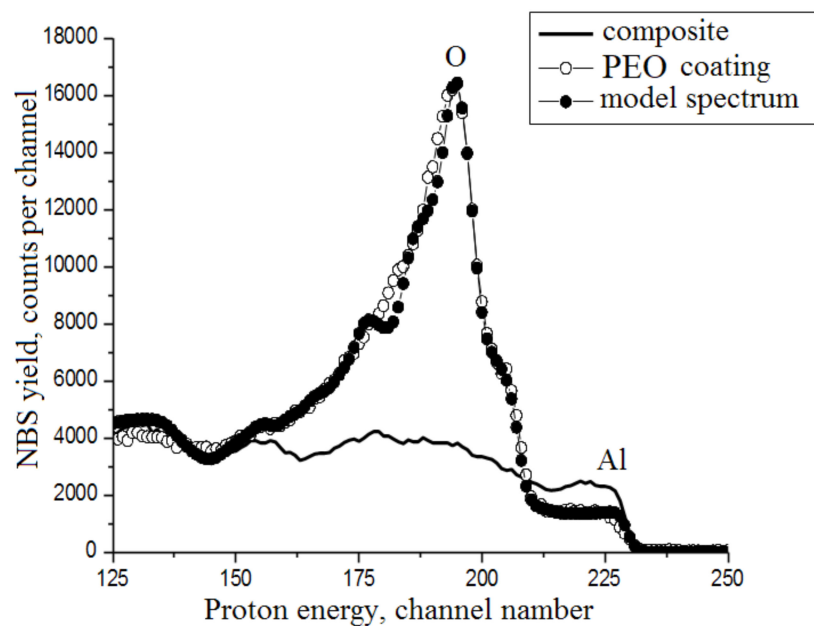
Figure 4. Experimentally measured and calculated nuclear backscattering (NBS) spectra of 7.4 MeV protons for the coating formed by 60 mins of PEO on the composite Al + 1% Cu.

NBS simulation showed the decrease in oxygen content when approaching the barrier layer of the PEO coating. When modeling NBS, PEO coatings were represented by three layers, with different ratios of aluminum to oxygen. The first layer corresponded to Al_2O_3 oxide and its thickness was 17, 23, and 13 μm for the PEO coatings on the Al, Al + 1% Cu, and Al + 4.5% Cu composites, respectively. The second layer, with the thickness of ~9 μm, for the PEO coatings on all composites contained metal inclusions, with a predominance of Al_2O_3. The third layer was characterized by an elevated aluminum content and its thickness was 12, 10, and 9 μm for the PEO coatings on the Al, Al + 1% Cu, and Al + 4.5% Cu composites, respectively. Note that NBS spectrometry gives a mass thickness, i.e., the porosity of the coating is not considered [10,25].

The increased aluminum content in the second layer of the PEO coatings may be due to the inclusions of the aluminum composite that have been incorporated into the coating structure during the PEO treatment. Sufficiently thick oxide films on the grain boundaries impede oxidation of these inclusions. The composition of the third layer may be also due to an unevenness of the coating thickness (about 10 μm).

For PEO coatings formed during 180 min, NBS-analysis showed that the layers, with a thickness of more than 50 μm, completely corresponded to the oxide without metallic inclusions. Thus, the increase of the PEO treatment duration leads to oxidation of residual metal inclusions inside of the coating.

3.6. X-ray Diffraction Analysis

X-ray diffraction analysis showed that the PEO coatings on aluminum composites consisted of γ-Al_2O_3 and η-Al_2O_3 phases, with broadened peaks (Figure 5a). Despite the presence of some amount of silicon in the outer layer, the reflections corresponding to its oxides were absent, which indicates its amorphous state. In the case of the coating on the Al + 4.5% Cu composite, the reflexes of mullite Al_2SiO_5 (Figure 5b) were observed. It should be noted that the CuO phase reflections were lacking in the X-ray diffraction pattern of the coating on the Al + 1% Cu composite, but appear in the case of the coating on the Al + 4.5% Cu composite. An increase in the duration of the PEO treatment of

up to 180 min led to formation of the α-Al_2O_3 and mullite to the γ-Al_2O_3 and η-A_2O_3 phases in the coating on the Al composite (Figure 5c). Reflexes of α-Al_2O_3 in the coatings diffraction patterns were noticeable after 1.5 h of the PEO treatment.
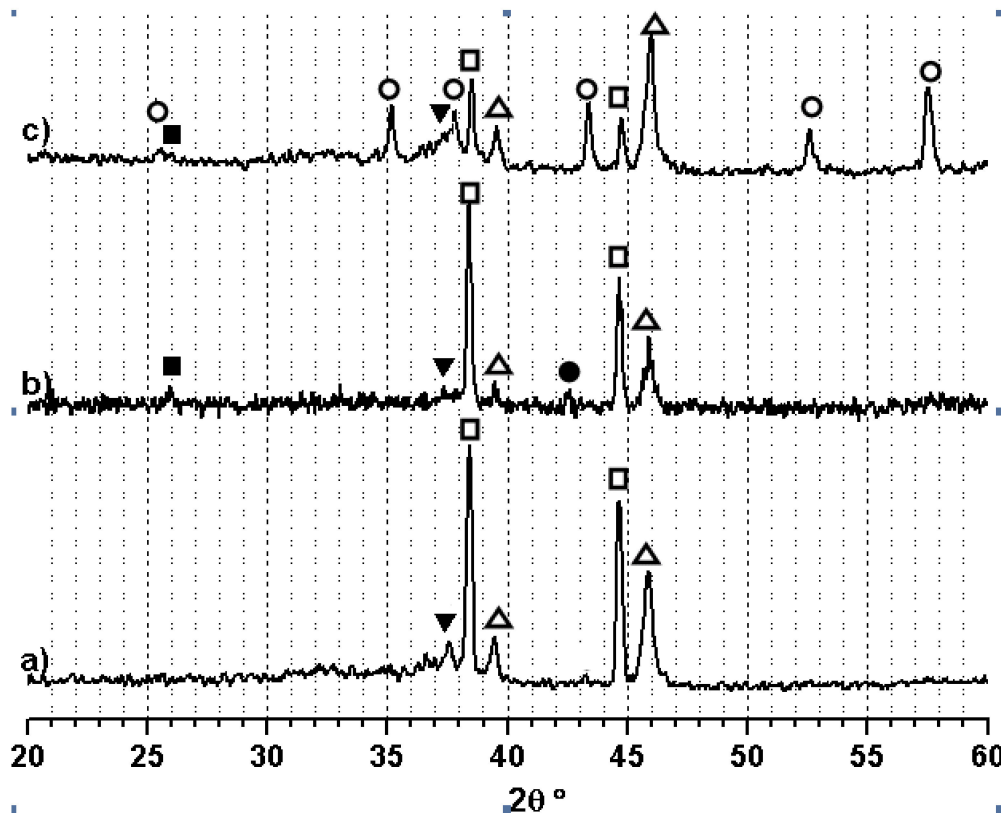
Figure 5. XRD patterns of the coatings formed on the composite, Al, for 60 min (**a**) and 180 min (**c**) of PEO and on the composite, Al + 4.5% Cu, formed for 60 min (**b**). □—Al; ○—α-Al_2O_3; Δ—γ-Al_2O_3; ▼—η-Al_2O_3; ●—CuO; ■—mullite.

3.7. Microhardness of PEO Coatings

Microhardness measurements were carried out on polished samples of the coatings' cross-section structure. The main layer of the coatings was analyzed. The coating microhardness for the composites, Al and Al + 1% Cu, obtained after 60 min of the PEO treatment, reached 12 GPa. The lower microhardness (9 GPa) was noted for the PEO coatings on the composite Al + 4.5% Cu. When the duration of the PEO treatment was increased to 180 min, the microhardness of the coating on the composite Al decreased to about 10 GPa. Herein, the initial microhardness of the composite Al is about 0.4 GPa.

### 3.8. Electrochemical Behavior of PEO Coatings

The polarization curves in Figure 6 illustrate that the PEO coatings in all cases "ennoble" (shift to the positive potential area) the steady-state electrode potential. The values of currents on all cathode and anode polarization curves for samples with PEO coatings were less than for that of the "bare" (uncoated) aluminum composites with and without copper, which indicates the coatings' protective properties.

It should be noted that the PEO coatings inhibit the anode process significantly more than the cathode one. At the same time, a change in the concentration of copper additions to aluminum composites within 1–3% did not significantly affect both the anode and cathode currents (Figure 6).

When copper was introduced into aluminum composites, the corrosion resistance became worse (curves 2′, 3′, 4′ in Figure 6). The smallest cathode currents (less by 1–2 orders of magnitude) and

anode currents (less by 2 orders of magnitude) were shown by the composite Al with PEO coating (curve 1′ in Figure 6). Alloyage of aluminum composites with copper increased the corrosion current density and PEO treatment, on the contrary, reduced it several times.
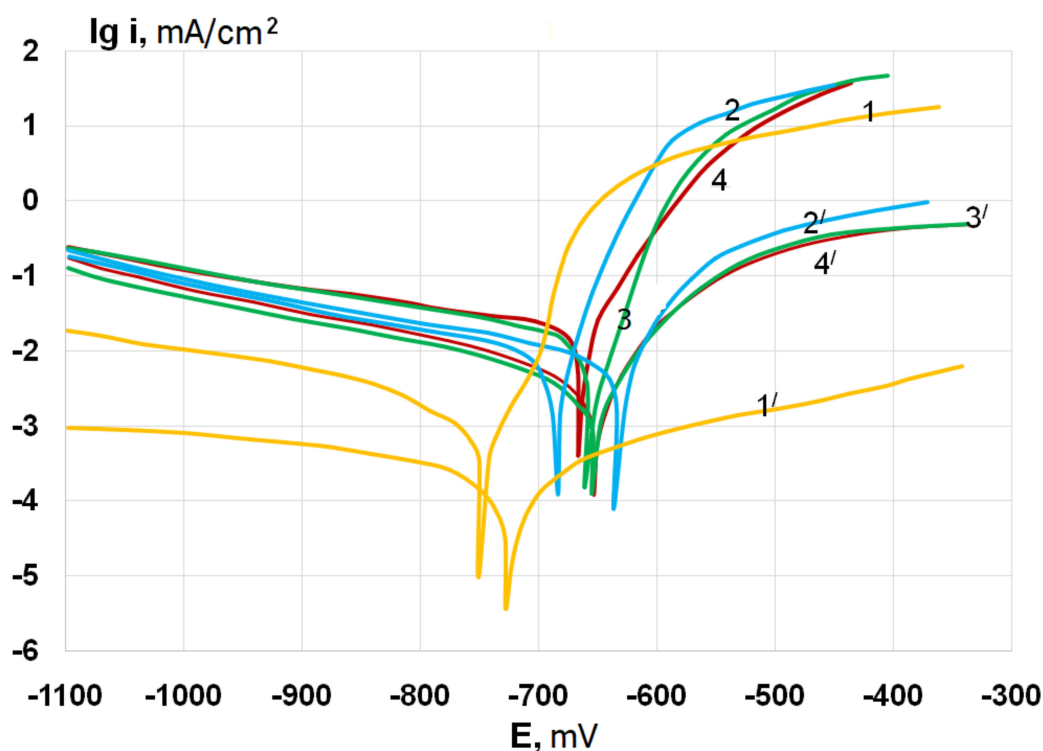
Figure 6. Polarization dependences of the current density, lg i, on the potential E in 3% NaCl solution at a potential sweep rate of 1 mV/s for the bare composites: Al (1); Al + 1% Cu (2); Al + 2% Cu (3); Al + 3% Cu (4) and the composites with PEO coatings: Al (1′); Al + 1% Cu (2′); Al + 2% Cu (3′); Al + 3% Cu (4′). All potentials are given relative to silver chloride electrode (Ag/AgCl).

A summary of the results of the potentiodynamic corrosion tests is given in Table 3. The corrosion current density of the PEO coated samples decreased relative to similar untreated alloys. Reducing the corrosion currents may indicate a protection effect of the PEO treatment on the corrosion rate of the electrodes, i.e., their corrosion rate should decrease in comparison with the samples without PEO coatings.

Table 3. The results of the potentiodynamic corrosion tests in 3% NaCl solution.

Composite	Al		Al + 1% Cu		Al + 2% Cu		Al + 3% Cu	
PEO coating	No	Yes	No	Yes	No	Yes	No	Yes
E_{corr}, mV(Ag/AgCl)	−751	−728	−684	−636	−661	−655	−667	−654
I_{corr}, mA/cm^2	2.5×10^{-3}	4×10^{-4}	8.9×10^{-3}	6.3×10^{-3}	1.5×10^{-2}	4.2×10^{-3}	1.8×10^{-2}	5.6×10^{-3}

4. Discussion

A three-layer structure of the PEO coating was noted on the cross-sections. However, comparison of the outer layer EDX data and the surface XPS data suggested the presence of an additional thin surface layer. This layer consisted mainly of electrolyte components (O, Si, Na, and K) and its thickness did not exceed 1 µm. The composition of this layer differs from that of the outer layer, containing impurities of silicon, but mainly consisting of alumina. Such a surface layer can be formed because of thermolysis of the electrolyte components in the microdischarges' action regions followed by the formation of their compounds with the coating material.

Unlike the PEO coatings formed on compact aluminum alloys in silicate-alkaline electrolytes (PEO duration up to 60 min) [10,11,34], coatings on aluminum composites contained only low-temperature modifications of alumina (γ, η-Al$_2$O$_3$). The η-Al$_2$O$_3$ peaks were broadened in XRD patterns. Their formation may be explained by the participation of the composite particles' oxide films in the PEO process.

The experiment results have shown a significant effect of copper concentrations in composites on the PEO process. So, the anodic voltage for the composites, with more than 2% Cu, reached the values observed for the composites without additives and 1% Cu, doped only at the end of the PEO process (~50 min). The presence of copper also affects the structure of the PEO coatings. In this case, a lower voltage of the PEO coating formation could lead to mullite crystallization due to a decrease in the spatial density of the microdischarges and the formation of silicon-enriched regions, which remain on the surface for a long time [34]. The nonuniformity of the coating thickness can be related to the uneven distribution of the copper dopants in the composite, whcih affected the rate of the PEO coating formation at different sections of the oxidation front. It can be assumed that, as the transition layer approaches the copper-containing inclusions, the rate of formation of the PEO coating increases due to their lower electrical resistance and higher thermal conductivity. However, inclusions of copper oxide in the PEO coating can lead to cracking because of a large difference in the thermal expansion with alumina. In the case of the Al + 1% Cu composite, copper-containing inclusions resulted in no significant thickness heterogeneity of the coatings, however, an increase in the rate of its formation was noted.

The structure of the PEO coating changes when the process duration is increased. EDX and NBS data have confirmed the absence of metallic inclusions in the coatings formed for 180 min of PEO. Anode voltage gradually rose as the duration of the process increased. In these cases, α-Al$_2$O$_3$ was found in the coatings. The formation of α-Al$_2$O$_3$ may be caused by an increasing of the local temperature in the microdischarges areas and, also, heat retention for a longer time due to worsening of the heat sink to the metal base and electrolyte because of the higher oxide layer thickness. In despite of the α-Al$_2$O$_3$ formation, the microhardness decreased in this coating, see paragraph 3.5. This may be due to a decrease in the density of the main coating layer caused by an increase of the channels' dimensions that exist in the coating in the process of microdischarge burning, cf [35].

In general, the microhardness of the investigated coatings were close to those given in the works devoted to PEO of aluminum composites. Thus, in [31], the microhardness of PEO coatings on copper-doped Al composites and 5–15% of dispersed particles of Al$_2$O$_3$ or SiO$_2$ decreased from 10 GPa at the boundary with the substrate to 6 GPa in the outer coating layer.

As for aluminum alloys, considered in [7–9], copper additives have impaired the corrosion resistance of the investigated composites. The corrosion current density of the PEO coated samples decreased several times for the aluminum composite compared to untreated alloys and slightly less for copper doped composites. This may be due to a change in the chemical composition (inclusions of copper oxide) and an increase in the porosity of the PEO coatings. The porosity can increase due to a change in the nature of the microarc discharges associated with the difficult growth of the forming voltage due to copper in the composites and copper is not a valve metal.

The corrosion characteristics of the investigated coatings, especially the microhardness, were close to those given in the works devoted to PEO of aluminum composites. In particular, the corrosion current density for the aluminum (0.1% Cu) composite was 3.09×10^{-3} mA/cm^2 for uncoated samples and 1.65×10^{-3} mA/cm^2 for the PEO coated samples [30].

5. Conclusions

After plasma electrolytic oxidation for 60 min, the coatings on aluminum composites contained metal inclusions. In such metal-ceramic coatings, the oxide was approximately a half of the whole coatings' volume. The process for powdered aluminum alloys was slower than for compact aluminum, which results in a slight increase in the thickness of the coatings, with a threefold increase in the treatment duration from 60 to 180 min. The presence of exclusively low-temperature modifications

of alumina γ-Al$_2$O$_3$ and η-Al$_2$O$_3$ in the coating composition after 60 min treatment was noted. The coatings formed for 180 min also contained high-temperature corundum α-Al$_2$O$_3$, and aluminum inclusions were absent. The electrochemical behavior of coated composites and uncoated ones in 3% NaCl was studied. The smallest cathode currents (less by 1–2 orders of magnitude) and anode currents (less by 2 orders of magnitude) were shown by the composite Al with coating. Alloyage of aluminum composites with copper increased the corrosion current density, while, on the contrary, plasma electrolytic oxidation reduced it several times.

Author Contributions: Conceptualization, A.B. and A.A. (Andrey Apelfeld); Formal analysis, S.S. and N.B.; Investigation, L.A., S.S., A.A. (Artem Ashmarin), K.A., N.T., M.G. and V.I.; Methodology, L.A., A.B. and A.S.; Software, K.A. and M.G.; Visualization, A.A. (Artem Ashmarin) and N.T.; Writing—original draft, S.S. and A.B.; Writing—review & editing, A.A. (Andrey Apelfeld).

Conflicts of Interest: The authors declare no conflict of interest.

References

1. Bodunrin, L.O.; Alaneme, K.K.; Chown, L.H. Aluminum matrix hybrid composite: A review of reinforcement philosophies; mechanical, corrosion and tribological characteristic. *J. Mater. Res. Technol.* **2015**, *4*, 434–445. [CrossRef]

2. Surappa, M.K. Aluminium Matrix Composites: Challenges and Opportunities. *Sadhana* **2003**, *28*, 319–334. [CrossRef]

3. Agureev, L.E.; Kostikov, V.I.; Yeremeyeva, Z.V.; Barmin, A.A.; Rizakhanov, R.N.; Ivanov, B.S.; Ashmarin, A.A.; Laptev, I.N.; Rudshteyn, R.I. Powder aluminum composites of Al–Cu system with micro-additions of oxide nanoparticles. *Inorg. Mater. Appl. Res.* **2016**, *7*, 687–690. [CrossRef]

4. Lurie, S.; Volkov-Bogorodskiy, D.; Solyaev, Y.; Rizahanov, R.; Agureev, L. Multiscale modelling of aluminium-based metal–matrix composites with oxide nanoinclusions. *Comput. Mater. Sci.* **2016**, *116*, 62–73. [CrossRef]

5. Kang, Y.C.; Chan, S.L.-I. Tensile properties of nanometric Al$_2$O$_3$ particulate-reinforced aluminum matrix composites. *Mater. Chem. Phys.* **2004**, *85*, 438–443. [CrossRef]

6. Ma, Z.Y.; Tjong, S.C.; Li, Y.L.; Liang, Y. High temperature creep behavior of nanometric Si$_3$N$_4$ particulate reinforced aluminium composite. *Mater. Sci. Eng. A* **1997**, *225*, 125–134. [CrossRef]

7. Aranda, B.; Cuevas, F.G.; Cintas, J.; Herrera-Garcia, M.; Urban, P. Effect of Copper Addition on Pitting Corrosion of MA-Al. *Acta Phys. Pol. A* **2016**, *129*, 788–791. [CrossRef]

8. Osório, W.R.; Freire, C.M.; Caram, R.; Garcia, A. The role of Cu-based intermetallics on the pitting corrosion behavior of Sn–Cu, Ti–Cu and Al–Cu alloys. *Electrochim. Acta* **2012**, *77*, 189–197. [CrossRef]

9. Na, K.-H.; Pyun, S.-I. Comparison of susceptibility to pitting corrosion of AA2024-T4, AA7075-T651 and AA7475-T761 aluminium alloys in neutral chloride solutions using electrochemical noise analysis. *Corros. Sci.* **2008**, *50*, 248–258. [CrossRef]

10. Apelfeld, A.V.; Belkin, P.N.; Borisov, A.M.; Vasin, V.A.; Krit, B.L.; Ludin, V.B.; Somov, O.V.; Sorokin, V.A.; Suminov, I.V.; Frantskevich, V.P. *Modern Technologies for Modification of Materials Surface and Formation of Protective Coatings. Volume 1: Microarc Oxidation*; Renome: Moscow-St.-Petersburg, Russia, 2017; pp. 345–438, (In Russian). ISBN 978-5-91918-832-2.

11. Yerokhin, A.L.; Nie, X.; Leyland, A.; Matthews, A.; Dowey, S.J. Plasma electrolysis for surface engineering. *Surf. Coat. Technol.* **1999**, *122*, 73–93. [CrossRef]

12. Nie, X.; Meletis, E.I.; Jiang, J.C.; Leyland, A.; Yerokhin, A.L.; Matthews, A. Abrasive wear/corrosion properties and TEM analysis of Al$_2$O$_3$ coatings fabricated using plasma electrolysis. *Surf. Coat. Technol.* **2002**, *149*, 245–251. [CrossRef]

13. Apelfeld, A.V.; Borisov, A.M.; Krit, B.L.; Ludin, V.B.; Polyansky, M.N.; Romanovsky, E.A.; Savushkina, S.V.; Suminov, I.V.; Tkachenko, N.V.; Vinogradov, A.V.; et al. The study of plasma electrolytic oxidation coatings on Zr and Zr-1% Nb alloy at thermal cycling. *Surf. Coat. Technol.* **2015**, *269*, 279–285. [CrossRef]

14. Curran, J.A.; Clyne, T.W. Porosity in plasma electrolytic oxide coatings. *Surf. Coat. Technol.* **2005**, *199*, 168–176. [CrossRef]

15. Vladimirov, B.V.; Krit, B.L.; Lyudin, V.B.; Morozova, N.V.; Rossiiskaya, A.D.; Suminov, I.V.; Epel'feld, A.V. Microarc oxidation of magnesium alloys: A review. *Surf. Eng. Appl. Electrochem.* **2014**, *50*, 195–232. [CrossRef]

16. Dehnavi, V.; Shoesmith, D.W.; Luan, B.L.; Yari, M.; Liu, X.Y.; Rohani, S. Corrosion properties of plasma electrolytic oxidation coatings on an aluminium alloy—The effect of the PEO process stage. *Mater. Chem. Phys.* **2015**, *161*, 49–58. [CrossRef]

17. Lesnevskiy, L.N.; Lyakhovetskiy, M.A.; Savushkina, S.V. Fretting wear of composite ceramic coating produced on D16 aluminum-based alloy using microarc oxidation. *J. Frict. Wear* **2016**, *37*, 268–273. [CrossRef]

18. Wang, K.; Kim, Y.J.; Hayashi, Y.; Lee, C.G.; Koo, B.H. Effects of electrolytes variation on formation of oxide layers of 6061 Al alloys by plasma electrolytic oxidation. *J. Ceram. Proc. Res.* **2009**, *10*, 562–566. [CrossRef]

19. Borisov, A.M.; Krit, B.L.; Lyudin, V.B.; Morozova, N.V.; Suminov, I.V.; Apelfeld, A.V. Microarc oxidation in slurry electrolytes: A review. *Surf. Eng. Appl. Electrochem.* **2016**, *52*, 50–78. [CrossRef]

20. Liu, C.; Liu, P.; Huang, Z.; Yan, Q.; Guo, R.; Li, D.; Jiang, G.; Shen, D. The correlation between the coating structure and the corrosion behavior of the plasma electrolytic oxidation coating on aluminum. *Surf. Coat. Technol.* **2016**, *286*, 223–230. [CrossRef]

21. Apelfeld, A.V.; Bespalova, O.V.; Borisov, A.M.; Dunkin, O.N.; Goryaga, N.G.; Kulikauskas, V.S.; Romanovsky, E.A.; Semenov, S.V.; Souminov, I.V. Application of the particle backscattering methods for the study of new oxide protective coatings at the surface of Al and Mg alloys. *Nucl. Instrum. Methods Phys. Res. B* **2000**, *161–163*, 553–557. [CrossRef]

22. Treviño, M.; Garza-Montes-de-Oca, N.F.; Pérez, A.; Juárez, A.; Colás, R.; Hernández-Rodríguez, M.A.L. Wear of an aluminium alloy coated by plasma electrolytic oxidation. *Surf. Coat. Technol.* **2012**, *206*, 2213–2019. [CrossRef]

23. Su, J.F.; Nie, X.; Hu, H.; Tjong, J. Friction and counterface wear influenced by surface profiles of plasma electrolytic oxidation coatings on an aluminum A356 alloy. *J. Vac. Sci. Technol. A* **2012**, *30*, 061402. [CrossRef]

24. Wang, K.; Sang, S.B.; Koo, B.H.; Wang, Y.Q.; Song, J. Tribological Properties of the Ceramic Coatings Prepared by Plasma Electrolytic Oxidation (PEO) on the Al 6061 Alloy. *Adv. Mater. Res.* **2010**, *123–125*, 1063–1066. [CrossRef]

25. Antipas, G.S.E. Augmentation of wear-protective coatings for non-ferrous alloys by the addition of Cr and Ni elements. *Mater. Res.* **2014**, *17*, 1485–1488. [CrossRef]

26. Abolhassani, A.; Aliofkhazraei, M.; Farhadi, S.S.; Rouhaghdam, S.A.; Asgari, M. Growth, corrosion, and wear study of nanocomposite PEO coating in electrolyte containing nickel sulfate. *J. Ultrafine Grained Nanostruct. Mater.* **2015**, *48*, 133–144. [CrossRef]

27. Wei, C.B.; Tian, X.B.; Yang, S.Q.; Wang, X.B.; Fu, R.K.; Chu, P.K. Anode current effects in plasma electrolytic oxidation. *Surf. Coat. Technol.* **2007**, *201*, 5021–5024. [CrossRef]

28. Matykina, E.; Arrabal, R.; Mohamed, A.; Skeldon, P.; Thompson, G.E. Plasma electrolytic oxidation of pre-anodized aluminium. *Corros. Sci.* **2009**, *51*, 2897–2905. [CrossRef]

29. Mingo, B.; Arrabal, R.; Mohedano, M.; Pardo, A.; Matykina, E. Corrosion and wear of PEO coated AZ91/SiC composites. *Surf. Coat. Technol.* **2017**, *309*, 1023–1032. [CrossRef]

30. Xia, L.-Q.; Han, J.-M.; Cui, S.-H.; Yang, Z.-Y.; Li, W.-J. Growth law and properties of ceramic coatings on SiCp/A356 composite fabricated by micro-arc oxidation. *J. Mater. Eng.* **2016**, *44*, 40–46. [CrossRef]

31. Morgenstern, R.; Sieber, M.; Lampke, T. Plasma electrolytic oxidation of AMCs. In *IOP Conference Series: Materials Science and Engineering*; IOP Publishing Ltd.: Bristol, UK, 2016; Volume 118.

32. Bespalova, O.V.; Borisov, A.M.; Vostrikov, V.G.; Romanovsky, E.A.; Serkov, M.V. Analysis of coatings and surface layers of materials by proton-backscattering spectrometry. *Phys. Nucl.* **2009**, *72*, 1664–1671. [CrossRef]

33. Feldman, L.C.; Mayer, J.W. *Fundamentals of Surface and Thin Films Analysis*; North-Holland: New York, NY, USA; Amsterdam, The Netherlands; London, UK, 1986; pp. 24–48. ISBN 0-444000989-2.

34. Dehnavi, V.; Liu, X.Y.; Luan, B.L.; Shoesmith, D.W.; Rohani, S. Phase transformation in plasma electrolytic oxidation coatings on 6061 aluminum alloy. *Surf. Coat. Technol.* **2014**, *251*, 106–114. [CrossRef]

35. Wang, K.; Koo, B.-H.; Lee, C.-G.; Kim, Y.-J.; Lee, S.-H.; Byon, E. Effects of electrolytes variation on formation of oxide layers of 6061 Al alloys by plasma electrolytic oxidation. *Trans. Nonferrous Met. Soc. China* **2009**, *19*, 866–870. [CrossRef]